
Systematic variation in osteoblast adhesion and phenotype with substratum surface characteristics

Jung Yul Lim,¹ Xiaomei Liu,² Erwin A. Vogler,^{2,3} Henry J. Donahue¹

¹Musculoskeletal Research Laboratory, Center for Biomedical Devices and Functional Tissue Engineering and Department of Orthopaedics and Rehabilitation, College of Medicine, Pennsylvania State University, Hershey, Pennsylvania 17033

²Department of Bioengineering, Materials Research Institute and Huck Institute for Life Sciences, Pennsylvania State University, University Park, Pennsylvania 16802

³Department of Materials Science and Engineering, Materials Research Institute and Huck Institute for Life Sciences, Pennsylvania State University, University Park, Pennsylvania 16802

Received 10 February 2003; revised 3 September 2003; accepted 10 September 2003

Abstract: Time-varying interactions of human fetal osteoblastic cells (hFOB 1.19) with materials of diverse chemical composition and surface energy, including biodegradable lactide/glycolide-based polymers, were assessed using a combination of assays sensitive to different phases of cell-substratum compatibility. Short-term (minutes to hours) cell-attachment-rate assays were used to measure the earliest stages of cell-surface interactions leading to adhesion. Proliferation-rate assays quantifying viability of attached cells were applied as a measure of medium-term (hours to days) cytocompatibility. Both attachment- and proliferation-rate assays were found to strongly correlate with material surface energy, with the exception of a reproducible and significant adhesion preference for fully water-wettable quartz over glass. No such adhesion/proliferation prefer-

ence was observed for hydrophobized counterparts, and attachment to water-wettable glass was significantly less than that to control tissue culture polystyrene. These results suggest that the amorphous SiO_x surface was inhibitory to hFOB 1.19 growth whereas putatively crystalline quartz stimulated bioadhesion. Alkaline phosphatase activity was evaluated as a marker for long-term (days) differentiation of hFOB 1.19 cells and did not strongly correlate with surface energy or, in the case of biodegradable polymers, chemical composition. © 2003 Wiley Periodicals, Inc. *J Biomed Mater Res* 68A: 504–512, 2004

Key words: osteoblast; adhesion; proliferation; surface energy; surface chemistry; biodegradable polymers

INTRODUCTION

Interaction of bone and cartilage cells (osteoblasts, osteoclasts, osteocytes, chondrocytes, etc.) with orthopedic biomaterials is of significant interest in development of structure-property relationships linking material characteristics (bulk composition, crystallinity, surface chemistry/energy, etc.) with cell phenotypic behavior (adherence, proliferation rates, differentiation, etc.). Much of the available information of this

kind for hard-tissue (bone) cells has been obtained with osteoblasts (bone accreting) because primary cells are relatively easy to sustain *in vitro*^{1–4} and several continuous cell lines are commercially available (e.g., hFOB 1.19, human fetal osteoblast ATCC CRL-11372; conditionally immortalized with a gene encoding for a temperature-sensitive mutant to A58 of the SV40 large T antigen).⁵ Likewise, primary chondrocytes are relatively easy to prepare from primary explants. This is in sharp contrast to osteoclasts (bone resorbing) that must be derived from hematopoietic stem cells and committed to an osteoclastic-development pathway *in vitro*^{6,7} or osteocytes that, despite being the most abundant cells in bone, are relatively difficult to isolate and culture *in vitro* and of which only a few well characterized established cell lines exist. Although good osteoblast and chondrocyte cell models are readily available, relatively few studies systematically correlating cell behavior with material properties have been reported.⁸ Moreover, there is

Correspondence to: H. J. Donahue; e-mail: hdonahue@psu.edu

Contract grant sponsor: Korea Science & Engineering Foundation (KOSEF) Post-Doctoral Fellowship Program

Contract grant sponsor: The Pennsylvania State Tobacco Settlement Formula Fund

Contract grant sponsor: The Pennsylvania State University Materials Research Institute

some inconsistency within the literature on this subject. For example, Ishaug-Riely et al.⁹ have reported little variation in chondrocyte phenotypic behavior with varying material characteristics, whereas a recent review of cytocompatibility studies reports a range of responses to different materials.⁸

Complexity of the cell adhesion process that spans a broad range of time and length scales no doubt contributes to some, if not most, of the differences among reports of cell interaction with materials. Adhesion of anchorage-dependent mammalian cells is traditionally viewed as occurring through at least four major steps that precede proliferation: protein adsorption, cell-substratum contact, cell-substratum attachment, and cell adhesion/spreading.^{8,10-15} Protein adsorption is complex in its own right, involving molecular-scale interactions with a hydrated surface^{16,17} that transpire over a short time frame relative to the full cell adhesion process. Cell contact and attachment involves gravitation/sedimentation to within 50 nm or so of a surface whereupon physical and (bio)chemical forces conspire to close the cell-surface distance gap. Attached cells then slowly (typically within hours) spread over the surface, pending compatibility with the surface, expressing a strong "biological component of adhesion"¹¹ that includes extrusion of extracellular matrix. Needless to say, (protein) composition of the fluid phase can greatly affect the entire bioadhesion process.^{12,13,18-21}

Thus, comprehensive assessment of cytocompatibility requires a combination of assays that are sensitive to the various stages of cell-material interaction outlined above. We report herein one such combination of methods applied to hFOB 1.19 cells using attachment/proliferation rate assays that are sensitive to early stages of bioadhesion (minutes to days, respectively) and measurement of alkaline phosphatase activity that is a marker for hFOB 1.19 differentiation over longer culture intervals (days to weeks). Substratum materials with varying surface properties include biodegradable polyglycolide and polylactide copolymers of general interest to the tissue-engineering field.

MATERIALS AND METHODS

Cells and cell culture

hFOB 1.19 (hFOB) cells were propagated (at the Musculoskeletal Research Laboratory, Penn State College of Medicine) in standard tissue culture polystyrene (TCPS) dishes from a stock supplied by Dr. Steven Harris (Bayer, West Haven, CT).⁵ Cells were sustained in a standard cell-culture incubator at 37°C and 5% CO₂ using Dulbecco's modified Eagle medium-Ham's F-12 (1:1) basal media supplemented with 10% charcoal-stripped fetal bovine serum, 1% penicil-

lin-streptomycin, 10⁻⁸M menadione, 100 µg/mL ascorbic acid, and 10⁻⁸M 1,25-dihydroxy vitamin D₃. These supplements followed the so-called differentiation media used in the original study of Harris et al.⁵ who developed the hFOB 1.19 cell line. Cells were used in assays described below before passage 20. Substantially identical short-term attachment assay results were obtained with hFOB from the same source independently propagated (at the Biomaterials Surface Science Laboratory, Penn State University) in the same medium mix but without penicillin-streptomycin, menadione, ascorbic acid, and vitamin D₃. Cells were removed from TCPS and all other test surfaces reported herein by rinsing in phosphate-buffered saline (PBS, without Ca and Mg; Gibco) and incubating in trypsin solution (1X porcine; Sigma). All cell counts were determined by hemacytometry.

Biodegradable polymers

Biodegradable polymers listed in Table I were synthesized by a ring opening polymerization of corresponding monomers of L-lactide, glycolide, and caprolactone with a catalyst of stannous octoate and with an initiator of 1-dodecanol or 1,6-hexanediol.^{22,23} Synthesized polymers were dissolved in chloroform, precipitated in excess methanol, and vacuum-dried. Number-average molecular weight was measured by gel permeation chromatography (GPC).

Surfaces and surface treatments

Monolithic quartz and glass substrata in the form of microscope slides and coverslips, respectively, were rendered fully water-wettable by air-plasma-discharge treatment (13.56 MHz, 100 mtorr in a commercial inductively coupled plasma cleaner; Harrick, Ossining, NY) after 3× consecutive washings in fresh volumes of distilled water, isopropyl alcohol, and chloroform. Test surfaces thus prepared were shown to be fully water-wettable by visual examination of droplet spreading on these hydrophilic surfaces and, in the case of glass coverslips, direct measurement of water contact angle by Wilhelmy-plate tensiometry (using a Camtel CDCA model 100 tensiometer, Royston, UK). Cleaned and plasma-treated quartz and glass were hydrophobized by reaction with octadecyltrichlorosilane (OTS) at 5% (w/v) solution in chloroform at reflux temperature. OTS-treated substrata were rinsed 3× with fresh chloroform to remove nonreacted OTS, minimizing contact with air by keeping surfaces in chloroform vapor. Rinsed OTS-treated surfaces were dried in air before use.

Biodegradable polymer thin films were fabricated by spin casting at 1500 rpm for 30 s using a Cee Instruments programmable spin coater housed in a laminar-flow hood. Polymers were dissolved into 1.5–2.5% (w/v) chloroform solution, depending on intrinsic viscosity, and cast onto 22-mm glass coverslips. Visual and microscopic examination revealed smooth, contiguous, and pin-hole-free films. Thickness was not characterized.

Advancing and receding water contact angles were measured on test surfaces using a commercial automated tensi-

TABLE I
hFOB Adhesion and Proliferation to Materials with Varying Composition and Surface Energy

Surface	Contact Angle (Degrees)		Adhesion		Proliferation	
	Advancing	Receding	% I_{\max} (%)	$t_{1/2}$ (min)	k ($\text{h}^{-1} \times 10^2$)	t_d (h)
TCPS	55.0 \pm 1.5	45.0 \pm 0.8	55.3 \pm 2.5	31.0 \pm 2.8	2.23 \pm 0.02	34.0 \pm 0.4
Plasma-treated quartz (PTQ)	0 \pm 0.0	0 \pm 0.0	72.4 \pm 4.8	38.0 \pm 4.0	2.62 \pm 0.02	29.4 \pm 0.3
OTS-treated quartz (STQ)	112.7 \pm 1.7	98.1 \pm 0.8	10.6 \pm 2.7	78.5 \pm 6.5	1.14 \pm 0.06	63.9 \pm 3.2
Plasma-treated glass (PTG)	0 \pm 0.0	0 \pm 0.0	38.6 \pm 4.2	61.8 \pm 2.6	2.12 \pm 0.01	35.6 \pm 0.2
OTS-treated glass (STG)	105.9 \pm 0.4	97.1 \pm 2.7	18.5 \pm 2.9	72.7 \pm 4.1	1.41 \pm 0.01	52.3 \pm 0.4
PLGA 5/5 ($M_n = 80$ k)	71.0 \pm 1.8	56.9 \pm 2.4	32.6 \pm 2.5	64.6 \pm 4.1	1.91 \pm 0.02	39.4 \pm 0.5
PLGA 7/3 ($M_n = 96$ k)	73.5 \pm 2.2	64.4 \pm 1.8	23.2 \pm 2.5	69.3 \pm 5.0	1.70 \pm 0.02	43.7 \pm 0.4
PLA ($M_n = 160$ k)	78.0 \pm 0.8	66.3 \pm 0.6	13.8 \pm 2.3	72.6 \pm 4.1	1.33 \pm 0.02	55.3 \pm 1.0
PCL ($M_n = 80$ k)	76.6 \pm 1.2	68.8 \pm 4.9	8.2 \pm 1.7	74.8 \pm 2.8	1.08 \pm 0.02	67.2 \pm 1.1
PLCL 7/3 ($M_n = 82$ k)	77.0 \pm 0.7	68.3 \pm 0.5	11.8 \pm 2.6	71.1 \pm 3.1	1.25 \pm 0.04	58.5 \pm 1.8
PLGCL 2.5/2.5/5 ($M_n = 60$ k)	77.9 \pm 1.4	68.3 \pm 2.1	19.6 \pm 3.1	69.3 \pm 3.0	1.49 \pm 0.03	49.6 \pm 0.9
PLGCL 3.5/3.5/3 ($M_n = 54$ k)	66.3 \pm 6.2	58.4 \pm 3.8	23.1 \pm 2.1	68.5 \pm 3.6	1.64 \pm 0.02	45.3 \pm 0.5

The unit of variability for contact angle is standard deviation, whereas those for the adhesion and proliferation kinetics are standard errors of the curve fitting.

See Figure 1 for identification of adhesion and proliferation parameters.

M_n , number-average molecular weight by GPC; PLGA, poly(lactide-*co*-glycolide); PLCL, poly(lactide-*co*-caprolactone); PLGCL, poly(lactide-*co*-glycolide-*co*-caprolactone).

ometer (First Ten Angstroms Inc., Portsmouth, VA). The tensiometer used a Tecan liquid-handling robot to deposit 10 μL of distilled-deionized water (18 M Ωcm obtained from a Millipore Simplicity system; interfacial tension was checked periodically by Wilhelmy-balance tensiometry) onto a test surface supported on a rotary table housed in a humidified (>99% relative humidity) chamber. Droplets were viewed with magnifying cameras connected to a computer and images were continuously captured by a frame grabber at a programmable rate of 1 image/s while the rotary table was tilted at a rate of 1 $^\circ$ /min to a final tilt of 35 $^\circ$. Advancing and receding contact angles (θ) were monitored at 35 $^\circ$ tilt for 65 s as a check that wetting dynamics had come to steady state, with the average and standard deviation of the last 10 measurements reported in Table I. Advancing and receding water adhesion tension $\tau = \gamma_{lv} \cos\theta$ was computed from measured θ using $\gamma_{lv} = 72.8$ dyne/cm and applied herein as a measure of surface energy.^{11,24–26}

Assays

Short-term cell attachment assays were performed basically as described by Vogler and Bussian.²⁷ Briefly, hFOB cells were plated onto approximately 15 identically prepared surfaces that were placed under UV light for 60 min for sterilization with a single cell suspension diluted to approximately 2×10^4 cells/cm². Cells were allowed to adhere to the substrata for variable lengths of time in an incubator, selecting a single specimen for destructive analysis every 5 min from $0 < t < 30$ min, every 10 min from $30 < t < 60$ min, every 15 min for $60 < t < 120$ min, and every 30 min for $120 < t < 180$ min. At each time, substrata were rinsed with PBS and the attached cells were released with trypsin and counted. Adhesion assays were done three times each in triplicate.

Proliferation assays were set up basically in the same way as the short-term attachment assays above. After 3 h attach-

ment time, substrata were rinsed with PBS to remove non-adherent cells and refreshed with growth medium. Remaining adherent cells were allowed to proliferate for 6, 12, 24, 48, and 72 h. At each time, a specimen was destructively analyzed by removing adherent cells and counting by hemacytometry. Experiments were performed three times each in triplicate.

Alkaline phosphatase (AP) activity at 3, 6, 9, and 12 days of culture was measured using a chromogenic assay involving conversion of *p*-nitrophenyl phosphate to *p*-nitrophenol. Cells were seeded and allowed to proliferate as described above and, at each selected time point, cells were lysed by rinsing with PBS and Triton X-100. The lysates were subjected to two freeze-thaw cycles, after which AP reaction buffer (1:1 mixture of 0.75M 2-amino-2-methyl-1-propanol and 2 mg/mL *p*-nitrophenol phosphate; Sigma) was added and incubated at 37 $^\circ\text{C}$ for 15 min. This reaction mixture was combined with 0.1N NaOH in a 96-well plate where absorption was measured at 410 nm. Enzyme activity was estimated from a *p*-nitrophenol standard curve. AP activity was normalized to total protein which was measured using a DC protein assay kit (Bio-Rad). Experiments were conducted three times each in triplicate and means and standard deviations were reported.

Computations and statistics

Quantitative short-term attachment parameters % I_{\max} and $t_{1/2}$ (Fig. 1) were extracted from experimental data by non-linear fitting to a three-parameter logistic function as described previously.²⁷ Proliferation kinetic data were fit to an exponential growth law of the form % $I = \%I_{\max} \exp\{k(t - t_L)\}$, where k is the proliferation rate in inverse time unit and t_L is a lag-time constant set to 3 h. Doubling time t_d was computed from fitted parameters. Error reported in attachment and proliferation kinetic parameters are standard errors of the fit.

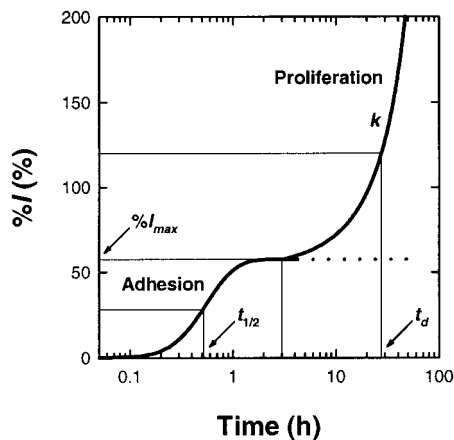


Figure 1. Schematic illustrating hFOB adhesion and proliferation identifying quantitative parameters extracted from the variation of percentage of a cell inoculum (%I) with time. $%I_{max}$ is the maximum percentage of a cell inoculum that adheres to a surface from a sessile cell suspension and $t_{1/2}$ measures half-time to $%I_{max}$. The proliferation rate (k) and cell-number doubling time (t_d) measure viability of attached cells.

Statistical significance was assessed by an analysis of variance followed by a Student-Newman-Keuls *post hoc* test to identify statistically significant differences between groups.

RESULTS AND DISCUSSION

We describe in this section the outcome of the different cytocompatibility assays applied in this work that are sensitive to different stages of bioadhesion (see Introduction), and then interpret these outcomes within the overall context of osteoblast-substratum interactions in Conclusions. First, short-term attachment rate assay results are disclosed that positively correlate with surface chemistry/energy.²⁷ This phase of cell-substratum interaction is crucial for anchorage-dependent cells such as osteoblasts because non-attached cells do not survive in suspension. Proliferation-rate results that measure vitality of adherent cells are compared with attachment rates and are found also to correlate with surface energy. Second, results of an AP assay that provides insights into cell differentiation dependence on substratum interactions are described. In contrast to adhesion/proliferation results, AP secretion is found not to strongly correlate with substratum surface energetics. Finally, we specifically focus on results obtained with biodegradable polymers that are of considerable interest in orthopedic tissue engineering.

Short-term cell adhesion and proliferation rates

Figure 1 diagrams the general form and characteristics of attachment and proliferation rate assays,¹¹⁻

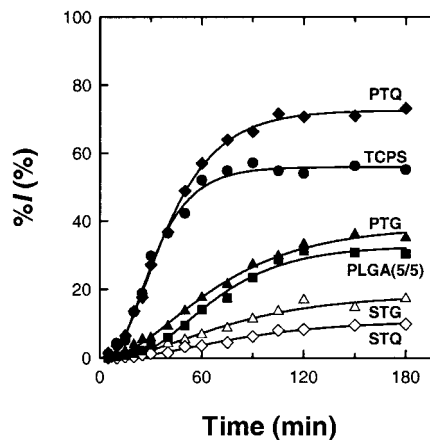


Figure 2. hFOB adhesion kinetics up to 180 min on various substrata (see Table I for material identification).

13,27 identifying quantitative parameters extracted by statistical fitting to data. $%I_{max}$ measures the maximum number of cells that attach to a surface from a sessile-liquid suspension, expressed as percent of inoculum. This number is estimated from a pseudo-steady-state adhesion plateau observed to occur for hFOB on all surfaces studied herein within a half-maximal attachment time $0 < t_{1/2} < 3$ h. After a significant dwell time, usually >3 h, cells divide at a rate measured by an exponential rate constant k and doubling time t_d . As will be shown subsequently, these parameters are characteristic of the substratum used in the attachment assay and, in this regard, hFOB behaves in a manner similar to that observed for soft-tissue cells (epithelioid and fibroblastic).²⁷⁻²⁹

Table I lists materials used in this study together with fitted parameters mentioned above. Parameter error estimates were derived from the previously explained nonlinear least-squares fitting to data such as that shown in Figures 2 and 3 that illustrate the full range of attachment and proliferation kinetics ob-

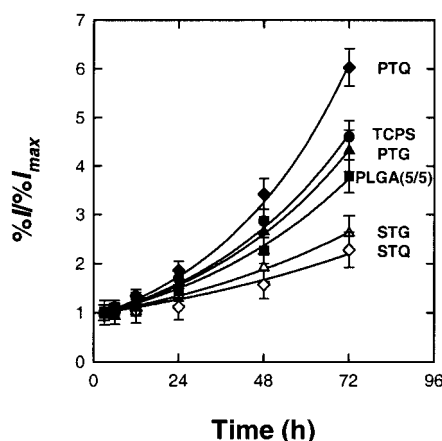


Figure 3. hFOB proliferation kinetics up to 72 h on various substrata (see Table I for material identification).

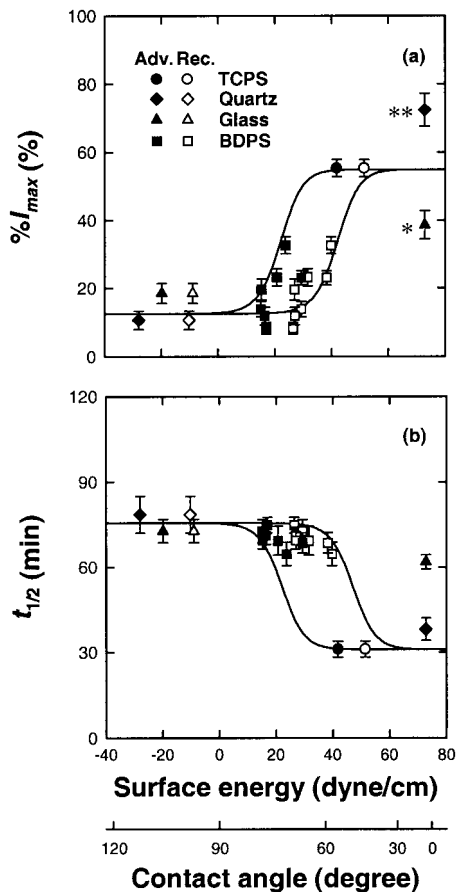


Figure 4. Correlation of % I_{\max} (a) and $t_{1/2}$ (b) with substrata surface energy as measured by water adhesion tension $\tau = \gamma_{lv}\cos\theta$, where $\gamma_{lv} = 72.8$ dyne/cm (see Fig. 1 for % I_{\max} and $t_{1/2}$; advancing = filled symbols, receding = open symbols, BDPS = biodegradable polymers). % I_{\max} of plasma-treated quartz (PTQ) (**) is significantly higher than those of TCPS and plasma-treated glass (PTG) (both $p < 0.001$), and % I_{\max} of PTG (*) is significantly lower than that of TCPS ($p < 0.001$), both by an analysis of variance followed by a Student-Newman-Keuls *post hoc* test.

served. It is evident from both graphical and quantitative analysis that attachment and proliferation data were reproducible with time. Figure 4(a,b) correlates % I_{\max} and $t_{1/2}$ with substratum surface energy expressed in terms of the water adhesion tension $\tau = \gamma_{lv}\cos\theta$ (water wettability). Relatively hydrophilic surfaces fall on the right side of the abscissa of Figure 4 whereas more hydrophobic fall on the left (hydrophobic and hydrophilic are relative terms used herein only as a qualitative measure of water wetting that will be more precisely defined below).³⁰ Two contact angles, so-called advancing and receding (with associated advancing and receding θ), are required to fully characterize surface wetting due to the phenomenon of contact angle hysteresis.¹¹ Consequently, adhesion data for each surface have been plotted for both wetting values, in a manner that effectively treats advancing and receding wetting as separate surfaces,^{25,26,30}

although it is important to stress that cells “see” only one macroscopic surface for each material listed in Table I. Trend lines to guide the eye have been drawn through advancing and receding data on Figure 4, both suggesting that attachment efficiency % I_{\max} was very low for relatively hydrophobic surfaces ($\tau < 20$ dyne/cm) and increased with substratum hydrophilicity in a manner similar to that reported for soft-tissue cells.²⁸ Contact angle hysteresis disappears as surfaces become progressively more hydrophilic,¹¹ leading to a single data point for the fully water-wettable ($\tau \sim 73$ dyne/cm) quartz and glass surfaces. Interestingly, for these surfaces, we observed a reproducible and significant adhesion preference for fully water-wettable quartz over fully water-wettable glass that was not observed for OTS-treated specimens. Furthermore, hFOB attachment to fully water-wettable glass was reproducibly less than that of less-wettable TCPS, whereas attachment to fully water-wettable quartz was significantly higher than TCPS.

We speculate that the observed hFOB attachment preference for quartz over TCPS (and glass) is due to putative crystalline order in the quartz surface that is presumably absent in molded plastic (and amorphous glass). Discrimination against glass (relative to quartz and TCPS) may be due to toxic effects sometimes associated with Pyrex and soda glass.^{31,32} However this attachment preference occurs, we note that epithelioid cell (MDCK) attachment is comparatively insensitive to substratum surface energy for $40 < \tau_{adv} < 73$ dyne/cm,^{28,29} suggesting that hFOB attachment response to glass and quartz is unique. Clearly, more studies are required to fully characterize hFOB adhesion relative to that of soft-tissue cells before any cogent interpretation can be made and definitive conclusions drawn in this regard.

Figure 4(b) shows that time-to-half-maximum attachment $t_{1/2}$ was sharply dependent on surface energy as well. As in Figure 4(a), trend lines have been drawn through advancing and receding data but, unlike % I_{\max} , we observed that $t_{1/2}$ was nearly constant for surfaces of $-40 < \tau_{adv} < 40$ dyne/cm, precipitously decreasing for more hydrophilic surfaces. As in Figure 4(a), a noticeable attachment preference for fully water-wettable quartz over fully water-wettable glass was observed in $t_{1/2}$. The collective interpretation of Figure 4(a,b) is that hFOB attachment is relatively “slow and low” on hydrophobic surfaces ($-40 < \tau_{adv} < 30$ dyne/cm) compared with relatively “fast and high” for hydrophilic surfaces ($30 < \tau_{adv} < 73$ dyne/cm). Attachment to fully water-wettable quartz is relatively faster and higher compared with fully water-wettable glass.

Figure 5(a,b) is constructed similarly to Figure 4(a,b) correlating proliferation rate k and doubling time t_d with substratum surface energy. hFOB clearly grew slowly on hydrophobic surfaces relative to hydro-

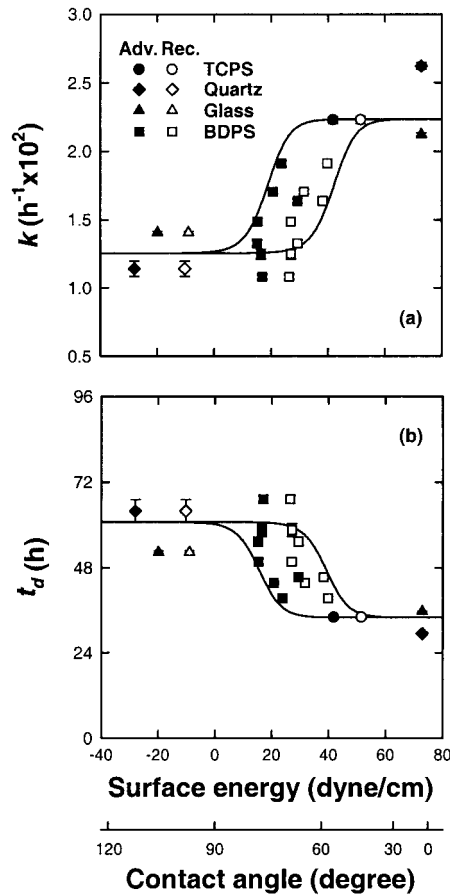


Figure 5. Correlation of k (a) and t_d (b) with substrata surface energy as measured by water adhesion tension $\tau = \gamma_{lv} \cos\theta$, where $\gamma_{lv} = 72.8$ dyne/cm (see Fig. 1 for k and t_d ; advancing = filled symbols, receding = open symbols, BDPS = biodegradable polymers).

philic surfaces with doubling time decreasing from about 60 h on surfaces exhibiting $-40 < \tau_{adv} < 30$ dyne/cm to 36 h for $30 < \tau_{adv} < 73$ dyne/cm. Proliferation preference for fully water-wettable quartz over fully water-wettable glass was not as pronounced as in short-term attachment rates, but close inspection of Figure 5 reveals a detectable difference between these two substrata and the TCPS control surface.

It is interesting that the hFOB spreading/proliferation phase of bioadhesion that occurs long after (>48 h) initial cell contact/attachment reflects substratum surface energy in a dose-response manner that is suggestive of a causal (rather than casual) relationship. Theory of short-term cell attachment has long implicated surface-energy effects from which correlations like those shown in Figure 4(a,b) can be qualitatively,^{14,33–38} if not quantitatively,^{11–13} understood. But relating surface physical chemistry to the activation of cell machinery responsible for replication is a much more daunting theoretical adventure for which we know of no literature reports. Nevertheless, latent surface-energy effects illustrated in Figure 4(a,b) for

hFOB are similar to previously reported results obtained with soft-tissue cells.^{39,40}

hFOB differentiation

We used AP activity as a measure of hFOB differentiation^{4,41} in long-term ($3 < t < 12$ days) contact with materials in Table I. Figure 6 simultaneously correlates AP activity with time in culture and substratum surface energy. Although statistically significant differences among materials studied were noted over the culture interval, no systematic dependence with surface energy energetics was observed. Thus, hFOB differentiation in long-term contact with selected substrata stands in stark contrast to short-term attachment- and proliferation-rate data described in the preceding section wherein $\%I_{max}$, $t_{1/2}$, k , and t_d were found to be highly correlated with surface energy as measured by τ .

Biodegradable polymers

Biodegradable polymers are popular candidates for tissue-engineering applications.^{8,9,41–45} A wide variety of compositions have been explored with considerable emphasis on glycolide, lactide, and caprolactone polymers, as well as co/ter-polymers thereof wherein composition variables can be tuned to achieve a balance of physical properties such as strength and degradability. As a consequence, we have examined performance of a few biodegradable polymer compositions listed in Table I. In general agreement with previous reports,⁹ biodegradable polymers prepared in thin-film form were substantially hydrophobic, exhibiting water con-

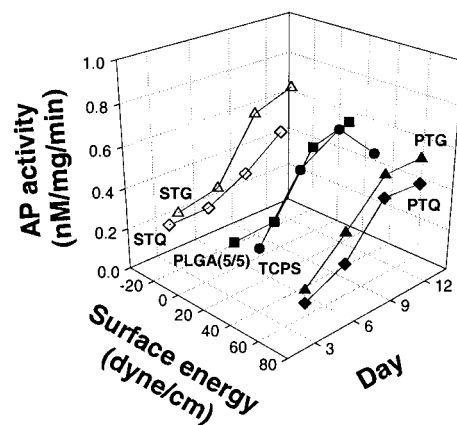


Figure 6. Variation in AP activity with substrata surface energy (as measured by advancing water adhesion tension $\tau = \gamma_{lv} \cos\theta$, where $\gamma_{lv} = 72.8$ dyne/cm) and as a function of culture time (see Table I for material identification).

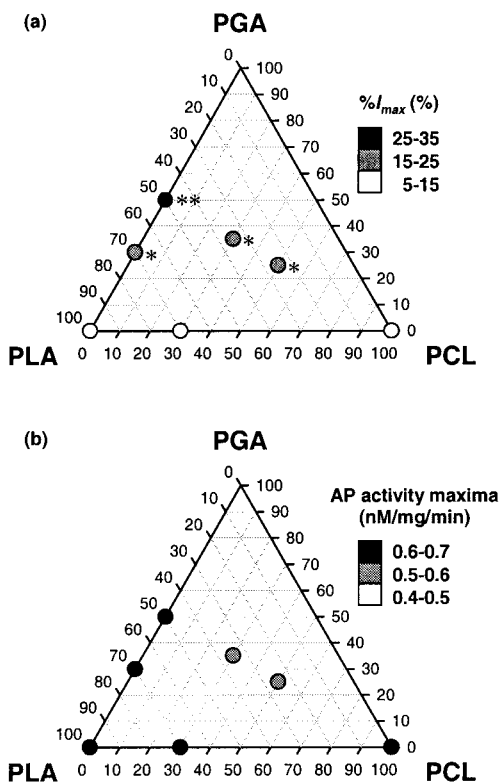


Figure 7. Ternary plots relating polyglycolide, polylactide, and polycaprolactone composition with $%I_{max}$ (a) (see Figs. 1 and 4) and maximal AP activity (b). In plot (a), $%I_{max}$ in black symbol (**) was significantly higher than those in white and gray symbols (both $p < 0.001$), and $%I_{max}$ in gray symbols (*) were significantly higher than those in white symbols ($p < 0.05$), both by an analysis of variance followed by a Student-Newman-Keuls *post hoc* test. In plot (b), the mean values did not show statistically significant differences in an analysis of variance.

tact angles of approximately 70° . As a consequence, hFOB attachment and proliferation data were grouped in a tight band shown in Figures 4 and 5 with little, if any, systematic differences in attachment and proliferation. Chondrocytes behave similarly in this regard,⁹ but unlike chondrocytes, hFOB expressed considerable adhesion preference for more hydrophilic substratum such as TCPS. Thus, we view hFOB interaction with biodegradable polymers as consistent with other materials that fall within a continuum of water wettability.²⁴

However, there were measurable differences among widely varying biodegradable polymer compositions (Table I) when viewed from the perspective of polymer chemistry. Figure 7(a,b) is ternary diagrams mapping cell response as measured by $%I_{max}$ and maximal AP activity onto composition. We contend that this kind of representation is somewhat more informative, from a materials science perspective, than bar graphs correlating biological response to polymer category or name that seem to dominate recent biomaterials literature (e.g., Ref. 9 and citations therein). Examination

of Figure 7(a) reveals that high polylactide (PLA) and polycaprolactone (PCL) compositions do not stimulate hFOB adhesion but that inclusion of polyglycolic acid increases hFOB adhesion 2–3-fold. Specifically, hFOB adhesion followed the order poly(lactide-*co*-glycolide) (PLGA) 5/5 > PLGA 7/3, poly(lactide-*co*-glycolide-*co*-caprolactone) > PLA, poly(lactide-*co*-caprolactone) 7/3, PCL. By contrast, AP activity maxima up to 12-day culture [Fig. 7(b)] was substantially independent of polymer composition, as was observed when correlated with surface energy (Fig. 6). Again, we note that hFOB differentiation in long-term contact with selected substrata stands in contrast to short-term attachment rates that were more sensitive to substratum composition.

CONCLUSIONS

The biological response to material surfaces that ultimately controls biocompatibility occurs through a sequence of events propagating from a surface along both spatial and temporal coordinates. The spatial coordinate ranges from the first few molecular layers surrounding the biology-contacting surface to macroscopic distances that delimit the boundaries of the host, defining local and systemic responses, respectively. The temporal coordinate varies from short-term or acute responses to long-term or chronic responses. These separate “components of biocompatibility” overlap in time and space in a manner that can cause subsequent events to partially or wholly obscure the preceding.⁴⁶ Thus, no single assay sampling a particular period of time or space can hope to resolve spatiotemporal components of biocompatibility. In the specific case of mammalian adhesion *in vitro*, short-term attachment rates sensitive to interfacial events affecting the earliest stages of cell-substratum compatibility^{12,13,27} and proliferation-rate assays measuring substratum effects on attached-cell vitality must be combined with longer-term measures of cell differentiation to obtain a complete picture of cytocompatibility.¹⁰ Application of one such combination of assays to osteoblastic cells (hFOB 1.19) described herein has revealed a strong correlation of attachment and proliferation with substratum surface energy in a manner paralleling that previously observed with soft-tissue cells (epithelioid and fibroblastic).^{28,29} However, for hFOB, a reproducible adhesion preference for fully water-wettable quartz over fully water-wettable glass was observed that was not evident for hydrophobized counterparts. Furthermore, hFOB attachment to fully water-wettable glass was reproducibly less than that to TCPS, whereas attachment to fully water-wettable quartz

was significantly higher than TCPS. Similar trends were evident in proliferation-rate data as well, suggesting that the water-wettable (presumably amorphous) glass SiO_x chemistry inhibits early stages of hFOB bioadhesion whereas the water-wettable (presumably crystalline) quartz SiO₂ chemistry stimulates hFOB bioadhesion, relative to TCPS.

Osteoblast interaction with broad composition range of glycolide/lactide/caprolactone biodegradable polymers prepared as thin films was compared with glass, quartz, and polystyrene surfaces. Data indicate that short-term hFOB interaction with biodegradable polymers broadly correlated with surface energy (water wettability) and was not different than comparison materials. Compositional variations were resolvable on a ternary diagram that showed adhesion preference for polyglycolic acid polymers over PLA/PCL polymers.

AP activity was used as a marker of hFOB cell differentiation and thus a measure of long-term compatibility with materials. In contrast to shorter-term assays, no clear correlation with either material surface energy or chemical composition was observed. Our tentative conclusion is that, given sufficient time, hFOB conditions substratum to optimize proliferative potential and, as a consequence, little difference was observed in AP secretion for hFOB grown on a diverse set of materials with widely varying surface energy/chemistry.

References

- Cowles EA, Brailey LL, Gronowicz GA. Integrin-mediated signaling regulates AP-1 transcription factors and proliferation in osteoblasts. *J Biomed Mater Res* 2000;52:725–737.
- Scotchford CA, Cooper E, Leggett GJ, Downes S. Growth of human osteoblast-like cells on alkanethiol on gold self-assembled monolayers: the effect of surface chemistry. *J Biomed Mater Res* 1998;41:431–442.
- Loty C, Sauiter JM, Loty S, Jallot E, Forest N. 55S bioglass promoted differentiation of culture rat osteoblasts and created a template for bone formation. *Bioceramics* 1998;11:327–330.
- Perizzolo D, Lacefield WR, Brunette DM. Interaction between topography and coating in the formation of bone nodules in culture for hydroxyapatite- and titanium-coated micromachined surfaces. *J Biomed Mater Res* 2001;56:494–503.
- Harris SA, Enger RJ, Riggs BL, Spelsberg TC. Development and characterization of a conditionally immortalized human fetal osteoblastic cell line. *J Bone Miner Res* 1995;10:178–186.
- Matsuzaki K. Osteoclast differentiation factor induces osteoclast-like cell formation in human peripheral blood mononuclear cell cultures. *Biochem Biophys Res Commun* 1998;246:199–204.
- Kurihara N, Chenu C, Miller M, Civin C, Roodman GD. Identification of committed mononuclear precursors for osteoclast-like cells in long-term human marrow cultures. *Endocrinology* 1990;126:2733–2741.
- Anselme K. Osteoblast adhesion on biomaterials. *Biomaterials* 2000;21:667–681.
- Ishaug-Riley SL, Okun LE, Prado G, Applegate MA, Ratcliffe A. Human articular chondrocyte adhesion and proliferation on synthetic biodegradable polymer films. *Biomaterials* 1999;20:2245–2256.
- Horbett TA, Klumb LA. Cell culturing: surface aspects and considerations. In: Brash JL, Wojciechowski PW, editors. *Interfacial phenomena and bioproducts*. New York: Marcel Dekker; 1996. p 351–445.
- Vogler EA. Interfacial chemistry in biomaterials science. In: Berg J, editor. *Wettability, surfactant science series*. Vol. 49. New York: Marcel Dekker; 1993. p 184–250.
- Vogler EA. A thermodynamic model of short-term cell adhesion *in vitro*. *Colloids Surf* 1989;42:233–254.
- Vogler EA. Thermodynamics of short-term cell adhesion *in vitro*. *Biophys J* 1988;53:759–769.
- Barngrover D. Substrata for anchorage-dependent cells. In: Thilly WG, editor. *Mammalian cell technology*. Boston: Butterworths; 1986. p 131–149.
- Grinnell F. Cellular adhesiveness and extracellular substrata. In: Bourne GH, Danielli JF, Jeon KW, editors. *International review of cytology*. Vol. 53. New York: Academic Press; 1978. p 67–145.
- Andrade JD. Principles of protein adsorption. In: Andrade JD, editor. *Surface and interfacial aspects of biomedical polymers: protein adsorption*. Vol. 2. New York: Plenum Press; 1985. p 1–80.
- Ramsden JJ. Puzzles and paradoxes in protein adsorption. *Chem Soc Rev* 1995;24:73–78.
- Teare DOH, Emmison N, Ton-That C, Bradley RH. Effects of serum on the kinetics of CHO attachment to ultraviolet-ozone modified polystyrene surfaces. *J Colloid Interface Sci* 2001;234:84–89.
- Lee JH, Lee HB. Platelet adhesion onto wettability gradient surfaces in the absence and presence of plasma proteins. *J Biomed Mater Res* 1998;41:304–311.
- Andrade JD. Interfacial phenomena and biomaterials. *Med Instrum* 1973;7:110–120.
- Yamada KM, Kennedy DW. Dualistic nature of adhesive protein function: fibronectin and its biologically active peptide fragments can autoinhibit fibronectin function. *J Cell Biol* 1984;99:29–36.
- Kowalski A, Duda A, Penczek S. Kinetics and mechanism of cyclic esters polymerization initiated with tin (II) octoate. 3. Polymerization of L,L-dilactide. *Macromolecules* 2000;33:7359–7370.
- Kricheldorf HR, Kreiser-Saunders I, Stricker A. Polylactones 48: SnOct₂-initiated polymerizations of lactide: a mechanistic study. *Macromolecules* 2000;33:702–709.
- Vogler EA. How water wets biomaterials. In: Morra M, editor. *Water in biomaterials surface science*. New York: John Wiley & Sons; 2001. p 269–290.
- Vogler EA. Practical use of concentration-dependent contact angles as a measure of solid-liquid adsorption. I. Theoretical aspects. *Langmuir* 1992;8:2005–2012.
- Vogler EA. Practical use of concentration-dependent contact angles as a measure of solid-liquid adsorption. II. Experimental aspects. *Langmuir* 1992;8:2013–2020.
- Vogler EA, Bussian RW. Short-term cell-attachment rates: a surface sensitive test of cell-substrate compatibility. *J Biomed Mater Res* 1987;21:1197–1211.
- Vogler EA. Structure and reactivity of water at biomaterial surfaces. *Adv Colloid Interface Sci* 1998;74:69–117.
- Vogler EA. Water and the acute biological response to surfaces. *J Biomater Sci Polym Ed* 1999;10:1015–1045.
- Vogler EA, Martin DA, Montgomery DB, Graper JC, Sugg HW. A graphical method for predicting protein and surfactant adsorption properties. *Langmuir* 1993;9:497–507.

31. Freshney RI. Culture of animal cells: a manual of basic technique. New York: Alan R. Liss; 1983.
32. Kruse PF, Patterson MK. Tissue culture: methods and applications. New York: Academic Press; 1973.
33. Marmur A, Ruckenstein E. Gravity and cell adhesion. *J Colloid Interface Sci* 1986;114:261–266.
34. Rutter PR. The physical chemistry of the adhesion of bacteria and other cells. In: Curtis ASG, Pitts JD, editors. *Cell adhesion and motility*. London: Cambridge University Press; 1980. p 103–135.
35. Bongrand P, Capo C, Depieds R. Physics of cell adhesion. *Prog Surf Sci* 1982;12:217–235.
36. Pethica BA. Microbial and cell adhesion. In: Berkeley RCW, Lynch JM, Melling J, Rutter PR, Vincent B, editors. *Microbial adhesion to surfaces*. London: Ellis Harwood; 1983. p 19–45.
37. Facchini PJ, Neumann AW, DiCosmo F. Thermodynamic aspects of cell adhesion to polymer surfaces. *Appl Microbiol Biotechnol* 1988;29:346–355.
38. Pethica BA. The physical chemistry of cell adhesion. *Exp Cell Res Suppl* 1961;8:123–140.
39. Schakenraad JM. Cell-polymer interactions [PhD thesis]. University of Groningen; 1987.
40. Schakenraad JM, Busscher HJ, Wildevuur CRH, Arends J. The influence of substratum surface free energy on growth and spreading of human fibroblasts in serum proteins. *J Biomed Mater Res* 1986;20:773–784.
41. Botchwey EA, Pollack SR, Lavine EM, Laurencin CT. Bone tissue engineering in a rotating bioreactor using a microcarrier matrix system. *J Biomed Mater Res* 2001;55:242–253.
42. Langer R, Vacanti JP. Tissue engineering. *Science* 1993;260:920–926.
43. Langer R. Biomaterials in drug delivery and tissue engineering: one laboratory's experience. *Acc Chem Res* 2000;33:94–101.
44. Service RF. Tissue engineers build new bone. *Science* 2000;289:1498–1500.
45. Chapekar MS. Tissue engineering: challenges and opportunities. *J Biomed Mater Res* 2000;53:617–620.
46. Williams DF. General concepts of biocompatibility. In: Black J, Hastings G, editors. *Handbook of biomaterial properties*. London: Chapman & Hall; 1998. p 481–488.